

COMPARATIVE CHEMICAL FUNCTIONALIZATION OF NANOCARBON SURFACES FOR BIOMEDICAL APPLICATIONS

*Aihui Yan, Bonnie W. Lau, Love Sarin, Kevin McNeil, Agnes B. Kane, and Robert H. Hurt
Brown University, Providence, RI 02912*

Introduction

Carbon nanotubes have been reported to penetrate cell membranes (Pantarotto et al., 2004; Kam et al., 2004). They can also deliver into the cells various therapeutic agents, including peptides (Pantarotto et al., 2004), proteins (Kam et al., 2004), nucleic acids (Kam et al., 2005) and multiple drugs (Pastorin et al., 2006), which would alone exhibit poor cellular penetration. There are several drawbacks to carbon nanotube-based drug delivery systems, however, such as the inherent hydrophobicity, easy entanglement and/or aggregation, and potentially toxic catalyst residues. Carbon nanoparticles with simple spherical geometry and high purity may overcome these disadvantages. In the past we have successfully synthesized a hydrophilic, biocompatible supramolecular carbon nanoparticle with variable particle sizes by aerosol pyrolysis of liquid crystal (LC) solutions. (Yan et al., 2006) Our preliminary studies with immortalized mesothelial cells show rapid uptake (< 3 hours) of these nanoparticles and no apparent cytotoxicity up to 72 hours. (Yan et al., 2006)

In this paper, we compared a variety of covalent and noncovalent surface modification schemes by applying them to our LC-derived carbon nanoparticle platform under development for cancer cell delivery. Competing techniques for hydrophilicity enhancement (oxidation by ozone, nitric acid; aryl-sulfonation) were quantitatively compared using carbon films as model systems. On the LC-derived carbon nanoparticles, we measured the zeta potential, surface charge, and aqueous dispersibility before and after treatments by aryl-sulfonation, poly-L-lysine (PLL) loading, phospholipid-polyethyleneglycol loading and annealing. We also investigated the effects of those treatments on cell uptake and cytotoxicity of the LC-derived carbon nanoparticle platform. A specific potential application in cancer therapy is described.

Experimental

Preparation of carbon nanospheres

A commercial ultrasonic nebuliser was fed with 0.01-0.5 wt-% indanthrone disulfonate aqueous solution. Fine droplets were carried by a 5 L/min flow of nitrogen, into a 1-inch-diameter quartz tube in a horizontal furnace at 700 °C. The particles were captured on a nucleopore polycarbonate filter. Some nanoparticles from 0.5 wt-% precursor solutions were further heated up to 2700 °C in a custom rapid thermal annealing device (Shim et al., 2000).

Surface modification of carbon materials

Selected LC-derived carbon films (Jian et al., 2005) were heated up to 1000 °C and then modified in three ways: (1) 10 wt-% nitric acid liquid-phase treatment at room temperature for hours; (2) 2 wt-% ozone/oxygen gas-phase treatment at room temperature for 10 min followed by desorption in nitrogen flow up to 1000 °C; (3) aryl sulfonation by immersing the films into an aqueous mixture of sulfanilic acid and sodium nitrite at 70 °C for hours, extensively rinsing the films by deionized water and then drying the films in air flow at 70 °C. The identical treatments were made on physical vapour deposition (PVD) carbon films (Yan et al., 2006) as the model for conventional carbon nanoparticles.

Selected LC-derived carbon nanoparticles from 0.5 wt-% indanthrone disulfonate solutions were first sterilized at 400 °C for 15 min in nitrogen flow and then modified in four ways (see Fig. 1): (1) sulfonation by exposure to the mixture of sulfanilic acid and sodium nitrite at 70 °C for 1 hour to introduce more negative surface charges; (2) loading of poly-L-lysine (PLL, M. W. = 1000-4000) by electrostatic interaction at room temperature to impart positive surface charge; (3) loading of carboxylic-terminated, phospholipid-poly(ethylene glycol) (DSPE-PEG-COOH, M. W. = 2849.54) by hydrophobic forces at room temperature to cover the particles with a biocompatible polymer brush layer; and (4) annealing in N₂ gas up to 1000 °C to decrease the hydrophilicity by destroying the surface functional groups.

Characterization

Scanning electron microscope (SEM) images were taken at 1-5 kV on a LEO 1570 VP equipped with a field emission gun. High-resolution transmission electron microscope (HRTEM) images and electron diffraction patterns were recorded at 200 kV on a JEOL 2010. Nitrogen vapour adsorption isotherms were determined using an AUTOSORB-1 (QUANTACHROME) at 77 K after sample outgassing overnight at 200 °C. Dynamic light

scattering (DLS) and zeta potential experiments were performed on a Zetasizer Nano-ZS 900. UV-vis light absorption spectra were recorded on a PerkinElmer Lambda 35 UV/VIS Spectrometer in the range of 200-600 nm. In a typical wetting experiment, 5 μ L of distilled water was dropped onto the test surface and the contact angle was monitored by an Infinity K2 long working-distance microscope.

Cellular uptake and toxicity

We studied the interactions of mesothelial cells with the LC-derived carbon nanoparticles from the 0.5 wt-% precursor solution. Crystalline silica particles used as a positive (toxic) control were obtained from Duke Scientific (Cat. No. 209, surface area: 24.3 ± 1.1 m²/g, average diameter: 2 μ m). Ozonated carbon black used as a negative (non-toxic) control was prepared by passing 2 wt-% ozone in oxygen through carbon black M120 (Cabot Corporation, primary particle size: 75 nm) for 10 min at room temperature. All materials were first baked at 250 °C for 18 hours to inactivate endotoxin, and then suspended in sterile phosphate buffered saline (PBS) as concentrated stock solutions that were sonicated for one hour before diluted to experimental doses.

For the cytotoxicity experiments, D7 (a pre-neoplastic mesothelial cell line) cells were plated on glass coverslips (area: 3.8 cm²) at a density of 3.6×10^4 cells/coverslip. Cells were allowed to attach to the glass overnight in a DMEM/F12 (Gibco/Invitrogen) media supplemented with 10% fetal bovine serum (FBS), insulin, transferrin, sodium selenite (ITS), epidermal growth factor (EGF), L-glutamine, sodium pyruvate, Medium 199, gentamycin and penicillin/streptomycin. Eighteen hours later, the cells were treated with the various doses of particulates in serum-free RPMI-1640 media with the same supplements as described above. Doses used were calculated as mass of material per area of the coverslip, and doses ranged from 0-25 μ g/cm².

At selected time points post-treatment (0, 3, 6, 12, 24 and 72 hours of exposure), the cells were incubated with 2 μ M Syto-10 and 2 μ M ethidium homodimer (Molecular Probes Live/Dead viability cytotoxicity kit, Cat. No. L-3224) for 15 minutes at room temperature while rocking. Coverslips were gingerly inverted onto a microscope slide over a drop of RPMI-1640 media, and imaged on a Nikon Eclipse E800 microscope with epifluorescence illumination. Images were taken from five pre-determined areas of each coverslip at a magnification of 100X. Cell counts were performed using MetaMorph Software (Molecular Devices), and percent viability was calculated by the number of viable green-labeled cells divided by the total number of cells (dead red-labeled cells plus viable green-labeled cells).

Results and discussion

Indanthrone disulfonate is a lyotropic LC with high carbonization yield of 60% at 700 °C. (Jian et al., 2005) LC-derived carbon nanoparticles from 0.5 wt-% indanthrone disulfonate solutions before and after surface functionalizations are shown in Fig. 1.

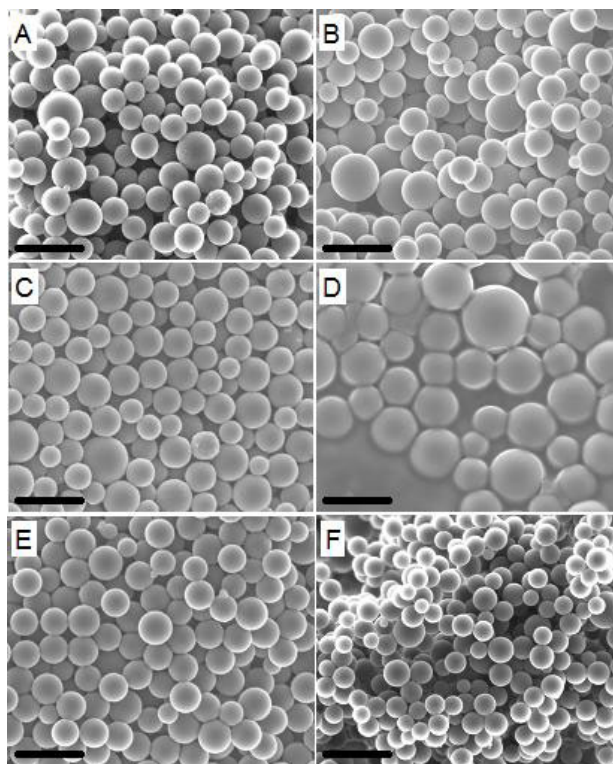


Figure 1. SEM images of surface modified LC-derived carbon nanoparticles. (A) As prepared carbon nanoparticles from 0.5 wt-% precursor solution; (B) after sterilization at 400 °C for 15 min in nitrogen flow; (C) after sulfonation at 70 °C for 1 hour; (D) after PLL loading (C:PLL = by weight); (E) after PEG loading (C:PEG = by weight); and (F) after annealing at 1000 °C for 2 min in nitrogen flow. The scale bar: 1 micron.

Use of 0.5 wt-% indanthrone disulfonate solutions leads to smooth spherical particles of a 500 nm typical diameter (Fig. 1A). At this length scale surface tension forces dominate to give the minimum area form (sphere) with no visible sign of indanthrone disulfonate crystals (Jian et al., 2005). The BJH surface area (Gregg and Sing, 1982; Lowell, 1979) measured by nitrogen vapor adsorption is 5.6 m²/g. Use of 0.1 wt-% solutions leads to nanoparticles of 250 nm typical diameter, which begin to show a polygonal crystal structure. Solutions of 0.01 wt-% yield 120 nm particles and there is no intrinsic lower limit to nano particle size by this process. By Eq. [1] these particle sizes imply an initial mean droplet size of 4 μm, and the observed concentration/size relationship is close to the 1/3 power dependence predicted by the conservation law.

$$D_{part} = \left(\frac{\rho_{soln} - YC}{\rho_{carbon}} \right)^{1/3} D_{drop} \quad [1]$$

where D is the diameter; ρ is the true material density; Y is the carbonization yield of indanthrone disulfonate; C is the concentration (w/w) of indanthrone disulfonate solution.

Post-synthesis heating at 2700 °C introduces a surface roughness pattern of ridge-like domains, which are likely remnants of the original rod-like supramolecular aggregates in the LC precursor. This inverted crystal form is much more reactive than the carbon black reference at all annealing temperatures studied (1000-2700 °C) despite the much higher physical surface area of carbon black (38 m²/g) compared to that of LC-derived nanoparticles (5.6 m²/g). (Yan et al., 2006)

Quantitative hydrophilicity measurements were carried out on smooth planar carbon films made from the same LC precursor and at the same carbonization conditions. Use of films allows water contact angles to be measured directly without the complications associated with the roughness and porosity in nanomaterials. The all-edge LC-derived carbon films were quite hydrophilic in the as-prepared state, showing a water contact angle of 52°. We attribute this to the combination of all-edge architecture and the low carbonization temperature (700 °C). Both nitric acid treatment and ozone treatment make the LC-derived carbon films more hydrophilic, and the lowest water contact angle is 26° (Fig. 2).

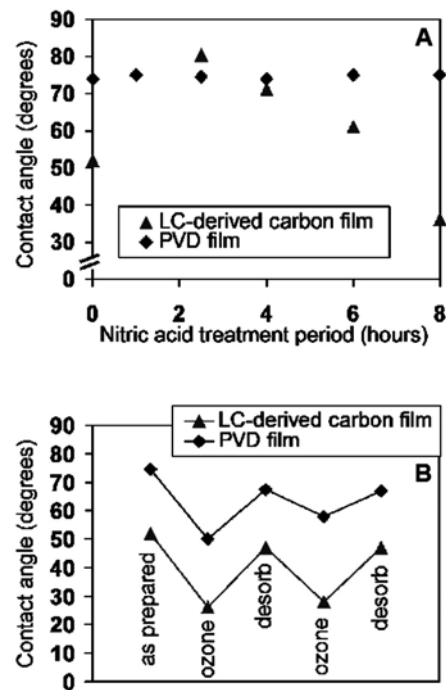


Figure 2. Water contact angles on carbon model films after nitric acid treatment and ozone treatment.

If even more hydrophilic behaviour is required for dispersion stability, we evaluated the use of sulfanilic acid treatment, and again used carbon films from the same precursor to obtain a quantitative measure. Treatment in the mixture of sulfanilic acid and sodium nitrite at 70 °C for 5 hours gave very low water contact angles (~5°). This high hydrophilicity implies that through reduction of diazonium ions carbon surfaces have been successfully decorated by $-\text{SO}_3^-$, which are fully dissociated and anionic at physiological pH.

Consistent with these film results is the observation that the LC-derived carbon nanoparticles treated by similar sulfonation process (see Fig. 1C) showed excellent aqueous dispersibility. Those nanoparticles self-dispersed into water, and the suspensions were stable up to 18 hours at room temperature. As to pristine LC-derived carbon nanoparticles, they could disperse into water by sonication and then began to settle down after 4 hours. Both of our LC-derived carbon nanoparticles are more hydrophilic and much easier to disperse than the carbon black used as a negative control in the toxicity tests.

The zeta potentials of LC-derived carbon nanoparticles were measured in various aqueous systems (0-0.01 M NaCl). Sulfonation increases the intrinsic negative charge on those carbon nanoparticles due to the known anionic character of the highly acidic sulfonate groups. According to Ohshima et al. (1982) and Attard et al. (2000), which deals with the relationship of the diffuse layer potential (nearly identical to the zeta potential (Attard et al., 2000)) and the real surface charge density, the as-prepared carbon nanoparticles possess a surface charge density of ~ 0.25 charge/nm². After pre-sterilization at 400 °C for 15 min, the surface charge density decreases to ~ 0.10 charge/nm², indicating that some surface charges have been destroyed. The subsequent 1-hour sulfonation, however, increases the surface charge density to ~ 0.60 charge/nm².

Positively charged LC-derived carbon nanoparticles (Fig. 1D) were obtained by mixing sterile LC-derived carbon nanoparticles with PLL at room temperature. The positively charged PLL is able to attach to intrinsically negative surface of sterile LC-derived carbon nanoparticles by electrostatic interaction. PLL is a cell-penetrating peptide that facilitates nanoparticle uptake through internalization process. (Fischer et al., 2005) Because of the strong affinity of cells toward PLL, free PLL in cell culture medium has been observed to attract adherent cells off the PLL-coated substrate in *in vitro* studies. To reduce the concentration of free PLL, it is desirable to wash PLL-carbon nanoparticles prior to cell studies. Fig. 3 shows the zeta potentials of PLL-carbon nanoparticles after several centrifugation-washing cycles. The zeta potential is ~ 35 mV in water when PLL:carbon $\geq 0.15\%$ by weight, and drops to -3.5 mV after 6 washes. For cell studies we selected the single wash process which removes some of the free PLL while keeping the high zeta potential ($+20$ mV) to aid in suspension stability.

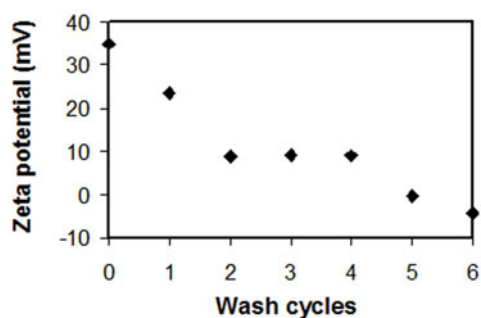


Figure 3. Zeta potentials of PLL-carbon nanoparticles in deionized water over the course of six wash cycles with deionized water to reduce the free PLL. The nanoparticle suspension concentration is 50 mg/L.

PEG is a biocompatible polymer that suppresses adsorption of plasma proteins and thus prevents reorganization by the mononuclear phagocyte system and enhances the retention time in the body. (Fee and Van Alstine, 2006) We chose DSPE-PEG-COOH as a coating model to study the cellular uptake of PEG-carbon nanoparticles shown in Fig. 1E. The zeta potential of those nanoparticles (in Fig. 4) first decreases from -42 mV to -84 mV with increase of PEG loading, followed by a slight increase. These large absolute values of the zeta potential aid in aqueous dispersibility.

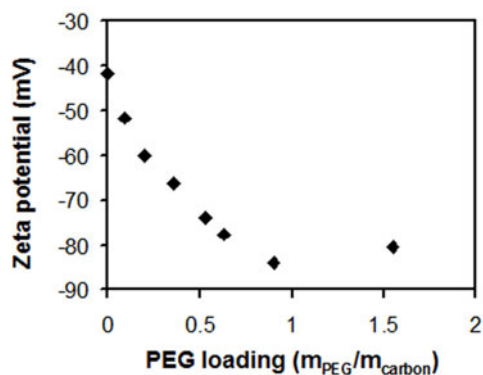


Figure 4. Zeta potentials of PEG-carbon nanoparticles in deionized water. The nanoparticle suspension concentration is 50 mg/L.

To assess the feasibility of LC-derived carbon nanoparticles in biological applications, samples from 0.5 wt-% precursor solution were further tested with D7 mesothelial cells for cytotoxicity measurement and cellular uptake. Those nanoparticles can be quickly taken up by the cells (within 3 hours) as shown in Fig. 5B. Quantitative toxicity tests (Figs. 5D,E) confirm that those particles have negligible cytotoxicity, with the cell death lower than 4% after a 72-hour post-treatment. Table 1 describes preliminary results from cell studies which assess comparative uptake and cytotoxicity on the various formulations of functionalized LC-derived carbon nanoparticles.

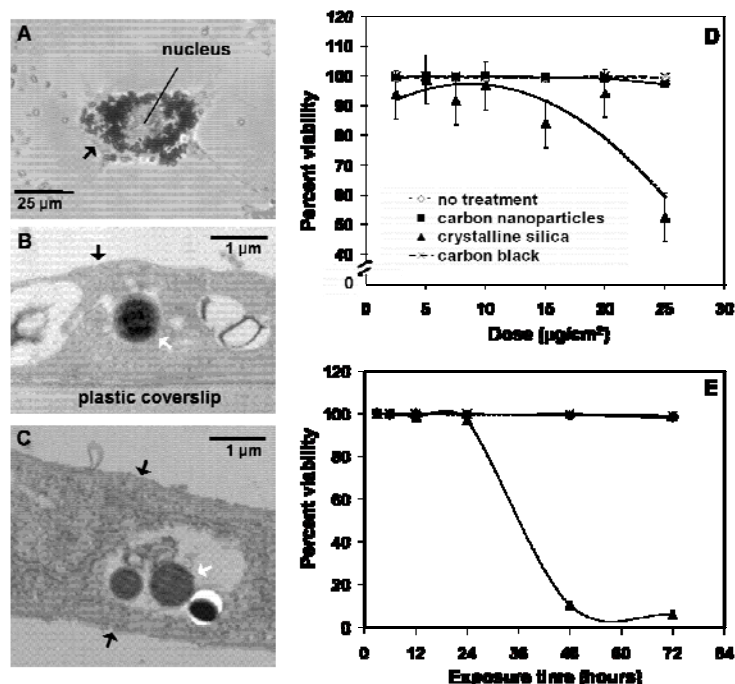


Figure 5. Evidence of cellular uptake and biocompatibility of LC-derived carbon nanoparticles. (A-C) Cellular uptake of LC-derived nanoparticles by mouse mesothelial cells with a dose of 10 µg/cm². (A) Phase contrast microscope image: 12 hours. (B) TEM image: 3 hours; and (C) TEM image: 6 hours. Black arrow: the cell; and white arrow: the carbon nanoparticles. (D) Cell viability with a dose range of 2.5-25 µg/cm² after 24 hours. (E) Cell viability with a fixed dose of 10 µg/cm² within 72 hours.

Table 1. Summary of nanoparticle uptake and cytotoxicity of a variety of modified LC-derived carbon nanoparticles with a dose of 10 µg/cm² after 72-hour exposure to mouse mesothelial cells.

carbon samples	charge	relative uptake	relative cytotoxicity
as-prepared nanoparticles	--	++	-
sulfonated nanoparticle	---	+++	-
PLL-carbon nanoparticles	++	++	++
crystalline silica	--	+	+++

Fig. 6 is an example of targeted delivery system based on LC-derived carbon nanoparticles. Elemental selenium (Se⁰), which is an essential trace in the body but shows toxic effects in marginally high doses, has been loaded onto as prepared LC-derived carbon nanoparticles by reducing sodium selenite by glutathione. (Sarin et al., 2007) The Se/C nanocomposite may be suitable for both *passive targeting* (through control over size, surface charge and hydrophobicity/hydrophilicity) and *active targeting* (by attaching an antibody/ligand).

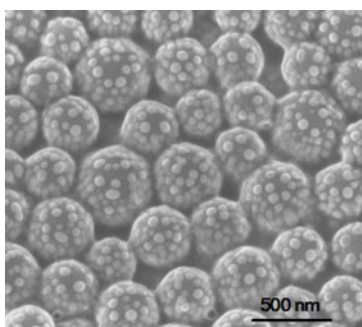


Figure 6. SEM image of LC-derived carbon nanoparticles from 0.5 wt-% precursor solutions doped with Se nanoparticles.

Conclusion

We have further developed a carbon nanoparticle platform for cell delivery by evaluating various treatments of the surface properties including aryl-sulfonation, PLL loading, PEG loading and annealing. These surface treatments increase the zeta potential well above the as-produced nanoparticles which provides more stable aqueous suspensions and higher surface charge densities for interaction with cell membranes and receptors. The preliminary cell studies showed that aryl-sulfonation accelerates nanoparticle uptake, while maintaining biocompatibility. On the other hand, positively charged PLL-carbon nanoparticles showed apparent cytotoxicity after 72-hour exposure to the mesothelial cells. Further work will examine covalent methods of achieving positive surface charge to avoid the free poly-lysine resulting from dynamic equilibrium with the physically adsorbed surface species.

Acknowledgements

Financial support was provided by the National Science Foundation, CTS-0342844, and the NIEHS-supported Superfund Basic Research Program at Brown University.

References

- Attard, P.; Antelmi, D.; and Larson, I. 2000. Comparison of the zeta potential with the diffuse layer potential from charge titration. *Langmuir* 16(4):1542-1552.
- Fee, C. J.; and Van Alstine, J. M. 2006. PEG-proteins: Reaction engineering and separation issues. *Chem. Engin. Sci.* 61(3):924-939.
- Fischer, R.; Fotin-Mleczek, M.; Hufnagel, H.; and Brock, R. 2005. Break on through to the other side-biophysics and cell biology shed light on cell-penetrating peptides. *Chem. Bio. Chem.* 6(12):2126-2142.
- Gregg, S. J.; and Sing, K. S. W. 1982. In *Adsorption, surface area and porosity*. Academic, New York, USA.
- Jian, K.; Xianyu, H.; Eakin, J.; Gao, Y.; Crawford, G. P.; and Hurt, R. H. 2005. Orientationally ordered and patterned discotic films and carbon films from liquid crystal precursors. *Carbon* 43:407-415.
- Kam, N. W. S.; Jessop, T. C.; Wender, P. A.; and Dai, H. 2004. Nanotube molecular transporters: internalization of carbon nanotube-protein conjugates into Mammalian cells. *J. Am. Chem. Soc.* 126(22):6850-6851.
- Kam, N. W. S.; Liu, Z.; and Dai, H. 2005. Functionalization of carbon nanotubes via cleavable disulfide bonds for efficient intracellular delivery of siRNA and potent gene silencing. *J. Am. Chem. Soc.* 127(36):12492-12493.
- Lowell, S. 1979. In *Introduction to powder surface area*. Wiley, New York, USA.
- Ohshima, H.; Healy, T. W.; and White, L. R. J. 1982. Accurate analytic expressions for the surface charge density/surface potential relationship and double-layer potential distribution for a spherical colloidal particle. *Colloid Interface Sci.* 90:17-26.
- Pantarotto, D.; Briand, J.-P.; Prato, M.; and Bianco, A. 2004. Translocation of bioactive peptides across cell membranes by carbon nanotubes. *Chem. Commun.* 1:16-17.
- Pastorin, G.; Wu, W.; Wieckowski, S.; Briand, J.-P.; Kostarelos, K.; Prato, M.; and Bianco, A. 2006. Double functionalization of carbon nanotubes for multimodal drug delivery. *Chem. Commun.* 11:1182-1184.
- Sarin, L.; Yan, A.; Sanchez, V.; Kane, A. B.; and Hurt, R. H. 2007. Carbon nanoparticles as a vehicle for cell delivery of nano selenium. Abstracts of Papers, 233rd ACS National Meeting, Chicago, IL, United States, March 25-29, 2007.
- Yan, A.; Lau, B. W.; Weissman, B. S.; Kulaots, I.; Yang, N. Y. C.; Kane, A. B.; and Hurt, R. H. 2006. Biocompatible, hydrophilic, supramolecular carbon nanoparticles for cell delivery. *Adv. Mater.* 18(18):2373-2378.
- Yan, A.; Xiao, X.; Kulaots, I.; Sheldon, B. W.; and Hurt, R. H. 2006. Controlling water contact angle on carbon surfaces from 5° to 167°. *Carbon* 44:3116-3120.